

Distant Cluster Hunting: A Comparison Between the Optical and X-ray Luminosity Functions from an Optical/X-ray Joint Survey

Megan Donahue¹, Jennifer Mack¹, Caleb Scharf^{1,2}, Paul Lee¹, Marc Postman¹, Piero Rosati³, Mark Dickinson¹, G. Mark Voit¹, John T. Stocke⁴

ABSTRACT

We present a comparison of X-ray and optical luminosities and luminosity functions of cluster candidates from a joint optical/X-ray survey, the ROSAT Optical X-ray Survey (ROXS). Completely independent X-ray and optical catalogs of 23 ROSAT fields (4.8 square degrees) were created by a matched-filter optical algorithm and by a wavelet technique in the X-ray. We directly compare the results of the optical and X-ray selection techniques. The matched-filter technique detected 74% (26 out of 35) of the most reliable cluster candidates in the X-ray-selected sample; the remainder could be either constellations of X-ray point sources or $z > 1$ clusters. The matched-filter technique identified approximately 3 times the number of candidates (152 candidates) found in the X-ray survey of the same sky (57 candidates). While the estimated optical and X-ray luminosities of clusters of galaxies are correlated, the intrinsic scatter in this relationship is very large. We can reproduce the number and distribution of optical clusters with a model defined by the X-ray luminosity function and by an $L_x - \Lambda_{cl}$ relation if $H_0 = 75 \text{ km s}^{-1} \text{ Mpc}^{-1}$ and if the $L_x - \Lambda_{cl}$ relation is steeper than the expected $L_x \propto \Lambda_{cl}^2$. On statistical grounds, a bimodal distribution of X-ray luminous and X-ray faint clusters is unnecessary to explain our observations. Followup work is required to confirm whether the clusters without bright X-ray counterparts are simply X-ray faint for their optical luminosity because of their low mass or youth, or a distinct population of clusters which do not, for some reason, have dense intracluster media. We suspect that these optical clusters are low-mass systems, with correspondingly low X-ray temperatures and luminosities, or that they are not yet completely virialized systems.

Subject headings: cosmology: observations — dark matter — galaxies: clusters: general — intergalactic medium — surveys — X-rays: galaxies

¹Space Telescope Science Institute, 3700 San Martin Drive, Baltimore, MD 21218, donahue@stsci.edu

²Columbia University, Dept. of Astronomy, Mail Code 5246 Pupin Hall, 550 W. 120th St., New York, NY 10027

³European Southern Observatory, Karl-Schwarzschild-Str. 2, Garching, D-85748

⁴University of Colorado, CASA, CB 389, Boulder, CO 80309

1. Introduction

X-ray and optical techniques for detecting clusters of galaxies each have their merits. Optical techniques have been in use for over four decades, and images of the optical sky are relatively inexpensive to obtain. New optical methods such as the matched-filter method (Postman et al. 1996, P96 hereafter) have allowed for automatic, uniform detection of optical overdensities of galaxies with magnitude distributions consistent with those of a typical cluster of galaxies. In the matched-filter method, fitting galaxy luminosity functions in addition to seeking overdensities of galaxies minimizes the projection effects that plagued earlier cluster cataloguing efforts. X-ray selection has the advantage of directly revealing the hot intracluster medium confined by the deep gravitational potential of the cluster. Since this emission is proportional to the gas density squared, and the X-ray sky is sparsely populated compared to the optical, X-ray detections have higher contrast and less contamination from physically unrelated systems. Early X-ray selection methods optimal for point sources (Gioia et al. 1990b) were biased somewhat towards selecting clusters with high central surface brightnesses, but there are now several algorithms optimized for detecting extended sources, including wavelets and Voronoi-Tesselation Percolation methods (Rosati et al. 1995; Scharf et al. 1997).

However, X-ray and optical studies of cluster evolution have progressed along separate paths. A decade ago, optical and X-ray surveys disagreed in their assessment of the amount of evolution clusters have experienced. Optical surveys indicated very little evolution since $z \sim 0.5 - 1$ (Gunn, Hoessel & Oke 1986) while X-ray studies suggested modest (Gioia et al. 1990a) to strong evolution (Edge et al. 1990, later retracted in Ebeling et al. 1997). The most recent X-ray samples of clusters over a range of redshifts out to $z \sim 0.8 - 1.2$ suggest that the X-ray luminosity function for moderate luminosity clusters has in fact not evolved significantly since $z \sim 0.8$ (Borgani et al. 1999; Nichol et al. 1999; Rosati et al. 1998; Jones et al. 1998), while the *most luminous* (and presumably most massive) systems, such as those contained in the EMSS, may have evolved somewhat (Gioia et al. 1990a; Henry et al. 1992; Nichol et al. 1997, Vikhlinin et al. 1998, 2000; Rosati et al. 2000; Gioia et al. 2001), but the community is not unanimous on this result (e.g. Jones et al. 1998). In contrast, recent optical surveys for distant clusters continue to find very little evidence for evolution (Couch et al. 1991; P96).

In an effort to establish the common ground between X-ray and optical studies of clusters and cluster evolution, we have undertaken a joint X-ray/optical survey to detect and study clusters of galaxies, called the ROSAT Optical X-ray Survey, or ROXS. In contrast to other ROSAT PSPC serendipitous surveys (e.g. Rosati et al. 1995, Jones et al. 1998, Romer et al. 2000, Vikhlinin et al. 1998), the ROXS team optically imaged the entire central 30' by 30' of each field in our survey. The X-ray selection and optical selection of cluster candidates were then determined independently. In this current work, we report results on the relation between the X-ray luminosity (L_x) and Λ_{cl} , a measure of the cluster's

optical luminosity. The ROXS has already been used to find a potential intergalactic X-ray filament (Scharf et al. 2000.) Paper II (Donahue et al., 2001) contains the catalogues, data reduction and observational details. For this paper we scale $H_0 = 75 h_{75}$ km/s/Mpc. We assume $q_0 = 0.5$ to ease comparison with earlier results.

2. Optical Observations and Analysis

We obtained the optical images with the prime focus camera T2KB at the Kitt Peak National Observatory 4-meter telescope March, 1996 and May, 1997. The 23 ROXS target fields were selected from a sample of archival ROSAT PSPC observations with exposure times of more than 8,000 seconds and Galactic latitude of > 20 degrees. Four 900-second, $16'$ by $16'$ exposures were obtained through the I-band filter, to tile the central $30'$ by $30'$ of each ROSAT field. Our 5σ detection limit of $I_{AB} = 24$ was sufficient to detect cluster galaxies 2 magnitudes fainter than the typical unevolved first-ranked elliptical at $z = 1$ (Postman et al. 1998). We constructed galaxy catalogs which were in turn used to build the optical cluster catalog. The matched filter method (P96), tuned to redshifts in the range $0.2 < z < 1.2$, was used to generate cluster catalogs in $\Delta z = 0.1$ intervals. Each cluster candidate is assigned a central position, radius (corresponding to the area of detection $= \pi r^2$), an estimated redshift, and a detection confidence (in units of σ). The algorithm also estimates an effective optical luminosity Λ_{cl} , which is the equivalent number of L^* galaxies in the cluster such that the optical cluster luminosity in units of solar luminosities is $L_{cl}/L_{\odot} = \Lambda_{cl}L^* = \Lambda_{cl}10^{-0.4(M_{\odot}-M^*)}$, where $M^* = -21.90 + 5 \log h_{75}$ in the I band (P96) and M_{\odot} is the absolute magnitude of the Sun. A K-correction is applied assuming a standard elliptical spectrum. For reference, a richness class 1 cluster at $z \leq 0.7$ has $\Lambda_{cl} = 30 - 65$ in the I-band (P96). Additional details regarding field selection, data reduction, and catalog construction for the galaxies and optical cluster candidates can be found in Paper II.

We defined 155 optical cluster candidates in 23 $30'$ by $30'$ fields, of which 142 satisfy a $\sigma > 3$ criterion. We computed a 4σ X-ray flux detection threshold within an aperture of $r = 1'$ centered on each optical candidate. We also computed the X-ray and optical selection functions for the survey (P96, Paper II).

3. X-ray Cluster Selection and Cross-Identification

A wavelet-based technique, described by Rosati et al. (1995), was used to create a catalog of X-ray clusters of galaxy candidates for each field observed at Kitt Peak. Several of these fields overlapped with the original RDCS (Rosati et al. 1995) sample, and thus the X-ray cluster candidates in many of the fields already have been confirmed and have

spectroscopic redshifts. The flux limits are approximately the same as those of the RDCS ($F_x > 10^{-14} \text{erg s}^{-1} \text{cm}^{-2}$). Fifty-seven X-ray candidate clusters and their associated X-ray parameters were found.

In order to define the optical/X-ray cross identifications we compared locations and contours of X-ray sources to contour maps of optical significance overlaid on the I-band image. Of the 57 X-ray candidates, 43 were located within our optical field of view and unobscured by scattered light or bright stars. Of the 43, 31 were visually identified with potential cluster candidates with $\Lambda_{cl} = 25 - 100$, of which 26 are very secure, with centroid separations of $\lesssim 1'$. Of the other 5, 3 are low-significance optical clusters ($\sigma < 3$) which were interesting because of their potentially high redshift, and two others are more distant affiliations of sprawling optical systems with a compact X-ray candidate. The remaining 12 X-ray cluster candidates can be divided into 4 *bona-fide* optically faint candidates, 6 candidates with very uncertain X-ray fluxes ($F_x/\sigma_{F_x} < 3$), one double source (likely to be two blended point sources), and one blend with the original ROSAT target. None of the optically-blank X-ray sources have yet been classified or confirmed at other wavelengths. Since the spurious fraction typical of the X-ray surveys is $\sim 10\%$ (Rosati et al. 1998; Vikhlinin et al 1998), ~ 6 of these sources are likely to be spurious or collections of point sources. Some of these candidates may be *bonafide*, albeit optically faint, high-redshift clusters. Near IR imaging might reveal such clusters. Ten X-ray candidates have confirmed spectroscopic redshifts; eight of these have estimated redshifts from the optical data that lie within $\Delta z = 0.1$ of the spectroscopic redshift (Paper II). Of the 142 optically selected candidates with $\sigma > 3$, 27 have X-ray counterparts (one has two counterparts). Up to 29 additional optical candidates have possible X-ray point-source counterparts within $1' - 2'$ which we do not use in our correlation analysis.

4. X-ray Luminosity (L_x) and Optical Luminosity (Λ_{cl}) Relationship

For a cluster in which mass traces optical light (M/L_{opt} is constant) and the gas is in hydrostatic equilibrium ($T \propto M^{2/3}$), and $L_x \propto T^3$ (empirical relation see e.g. David et al. 1993), we expect the X-ray luminosity to be related to the optical luminosity as $L_x \propto L_{opt}^2$. The empirical relationship between a cluster's X-ray luminosity and optical luminosity is not so well defined, in large part due to the difficulties inherent in measuring a cluster's optical luminosity and in getting a homogeneous set of total optical luminosities for a large number of clusters. Edge & Stewart (1991) found that the bolometric X-ray luminosity of a local sample of X-ray selected clusters correlated only very roughly with Abell Number and somewhat better with Bahcall galaxy density (number of bright galaxies within $0.5h^{-1}$ Mpc; 1977; 1981) for the smaller subsample (18) that had Bahcall galaxy densities. Arnaud et al.(1992) made a heroic effort to compute cluster optical luminosities at low redshift from a heterogeneous literature. The more systematic matched filter algorithm (P96) produces

Λ_{cl} , which is proportional to the estimated optical luminosity inside $1.5h_{75}^{-1}$ Mpc.

We plot the the relationship between bolometric L_x (in units of $10^{44}h_{75}^{-2}\text{erg s}^{-1}$) and Λ_{cl} for our sample of clusters of galaxies in Figure 1, including the 4σ upper limits for clusters for which there was no X-ray counterpart. We tested the relationship between L_x , Λ_{cl} and estimated z , including the upper limits for L_x , with a statistical procedure by Akritas & Siebert (1996) and Kembhavi, Feigelson, & Singh (1986) to test for partial correlation in the presence of censored data. Our aim was to see if L_x and Λ_{cl} were indeed correlated beyond the effect of z estimates on flux-limited surveys. We found that while the correlation between L_x and z is fairly strong, with a Kendall τ -coefficient of 0.6, the correlation between Λ_{cl} and z is not nearly as strong, $\tau = 0.037$, and the partial correlation of all 3 quantities is significant at the 95% level (Partial $\tau = 0.057 \pm 0.019$). The correlation between L_x and Λ_{cl} is $\tau = 0.0677 \pm 0.019$ (the same σ_τ for all τ , Kembhavi et al. 1986), and thus L_x and Λ_{cl} are correlated at the 3σ level.

We roughly fit a correlation of $\log L_{44} = (-3.6 \pm 0.7) + (1.6 \pm 0.4) \log \Lambda_{cl} - 2 \log h_{75}$, where $L_{44} = L_{x,bol}/10^{44}\text{erg s}^{-1}$, to the cross-identified X-ray/optical clusters using a method of bivariate correlated errors and scatter (Akritas & Bershadsky 1996) with bootstrap estimate of the variance, including intrinsic scatter. This fit is by no means a unique fit to the data, but it suits our purposes for the next discussion. The fit and scatter are also consistent with the upper limits, which are well mixed with the detections. The intrinsic scatter in the relation and the fit is significant.

5. The Λ_{cl} Function - X-ray Luminosity Function Comparison

We can compute the observed “ Λ_{cl} -Function” for these data from the estimates of Λ_{cl} , the selection function (a function of Λ_{cl} and redshift), and the effective sky coverage of the survey (4.84 square degrees). The maximum search volume as a function of Λ_{cl} is estimated for each cluster. (For details, see Paper II.) For a given Λ_{cl} , the $N(> \Lambda_{cl})$ is the sum over all $1/V_{max}(\Lambda_{cl})$ for which $\Lambda_{cl} > \Lambda$. We plot the differential function in Figure 2, binned such that each bin but the highest contains 9 clusters. This function is consistent with that derived from the much larger sample in the Deeprange survey (Postman et al, in preparation.)

We obtain a raw estimate of N at $\Lambda_{cl} \gtrsim 60$ of $\sim 1.3 \times 10^{-5}h_{75}^3 \text{ Mpc}^{-3}$, and $\Lambda_{cl} \gtrsim 80$ of $\sim 4 \times 10^{-6}h_{75}^3 \text{ Mpc}^{-3}$. The estimated value is consistent with the value for the Postman et al. (1996) survey at the same Λ_{cl} , ($\sim 4_{-2}^{+3} \times 10^{-6}h_{75}^3 \text{ Mpc}^{-3}$). The best fit differential Λ_{cl} function ($H_0 = 75$, $q_0 = 0.5$) is of the form:

$$\frac{dn}{d\Lambda_{cl}} = n_0 \left(\frac{\Lambda_{cl}}{40} \right)^{-\alpha} \quad (1)$$

where $\alpha = 5.3 \pm 0.5$ and $n_0 = 6_{-1}^{+3} \times 10^{-6}h_{75}^3 \text{ Mpc}^{-3}(\Lambda_{cl})^{-1}$. The uncertainties here do not

take into account the uncertainties on the survey volume, Λ_{cl} , or spurious fraction. Each (Λ_{cl}, z) data point is weighted equally in the fit and the influence of the spurious fraction is minimized by fitting only those 134 cluster candidates with $\Lambda_{cl} \geq 20$ and $\sigma \geq 3$.

Are the optical cluster candidates without X-ray counterparts spurious, real but X-ray faint clusters, or the high Λ_{cl} -tail of the more numerous low-mass, low- L_x X-ray clusters? We know already from spectroscopic followup of similar matched filter surveys that these clusters cannot all be spurious (Holden, et al. 1999; Adami et al 2000; Postman, Lubin & Oke 1998). We compare the Λ_{cl} function to the X-ray luminosity function (XLF) for 0.1 – 2.4 keV of the X-ray clusters of galaxies from the Brightest Cluster Survey (Ebeling et al. 1997) in order to answer this question.

A chain-rule conversion of the XLF to a Λ_{cl} function using the $L_x - \Lambda_{cl}$ relation fit in §3 produces a Λ_{cl} function significantly flatter than the observed Λ_{cl} function (Figure 2). If we simultaneously fit *both* the Λ_{cl} distribution function and the $L_x - \Lambda_{cl}$ relation, we obtain a steeper relation where $\log(L_{bol,44} h_{75}^2) = (-6.9 \pm 1.1) + (3.6 \pm 0.8) \log \Lambda_{cl}$, where the best-fit values of the slope and normalization are highly correlated. This relation, when used to convert the XLF to the Λ_{cl} function, results in a steeper Λ_{cl} function. We have also investigated the effect of a Gaussian distribution in Λ_{cl} with respect to L_x for the inferred Λ_{cl} function. The qualitative effect of scatter is to change the normalization but not the slope of the Λ_{cl} function.

The optical matched filter method detected many more cluster candidates than did the X-ray method, at thresholds optimal for maximizing the number of cross-correlated sources (Paper II). Our analysis demonstrates that at least one of the following three assumptions is false: (a) $L_x \propto \Lambda_{cl}^2$, (b) that we have accurately estimated the Λ_{cl} distribution function from the present dataset, and/or (c) that the X-ray luminosity function is accurately known. Of these three, (c) is most likely to be true, as several groups have obtained compatible results. The assumption (b) can be confirmed by an independent matched-filter survey (Deeprange, Postman et al. 1998). So (a) is the most likely weak link.

Our results are consistent with the hypothesis that all of the optical cluster candidates with $\Lambda_{cl} > 30$ are true clusters, as long as the true $L_x - \Lambda_{cl}$ relation is rather steep ($L_x \propto \Lambda_{cl}^{3.8 \pm 0.8}$). We do not need to assume that the optical candidates not detected in X-rays are X-ray faint yet massive clusters to explain our results here. However, if the $L_x - \Lambda_{cl}$ relation is indeed steeper than $\beta = 2$ and Λ_{cl} is directly proportional to L_{opt} , this result implies that the mass to light ratio of clusters continues to increase with the mass of the cluster, at least into the moderate mass range explored in our sample. We note that our survey is too small to include the most massive clusters, and our estimates of L_x and L_{opt} are confined to the central few arcminutes of each candidate. If $L_x \propto M^2$ at these mass scales, $M/L_{opt} \propto M^{1-2/\beta}$ for the range of cluster masses in our survey

($\sim 10^{14} - 10^{15} h_{75}^{-1} M_{\odot}$). This weak dependence of M/L on mass is not ruled out by existing data (e.g. Hradecky et al. 2000.)

Followup with weak lensing measurements, near-IR, and X-ray observations are essential. If the clusters are low-mass, the clusters with high Λ_{cl} but low L_x will have commensurately low X-ray temperatures. ROXS identifies optically rich examples of cluster candidates without extended X-ray counterparts for the assessment of the possible existence of optically bright but X-ray faint clusters of galaxies.

6. Summary

We have directly compared the results of cluster hunting with two competing methods: optical selection in the I-band, using the matched filter technique, and X-ray selection of extended sources. We have found that both methods reliably detect most of the richest, and presumably most massive systems, but the optical matched filter technique, because of the scatter and the steepness of the relation between X-ray and optical luminosities, produces more cluster candidates at our sensitivities. We present the first Λ_{cl} function for optically-selected clusters of galaxies. The Λ_{cl} function is consistent with the X-ray luminosity function for clusters of galaxies if the intrinsic, global $\Lambda_{cl} - L_x$ relation is consistent with that of the cross-identified candidates. In particular, we can explain our observations without appealing to an X-ray faint population of massive clusters of galaxies.

Predictions for an observational test using deep XMM-Newton/EPIC exposures based on our result are: (1) X-ray observations of the undetected, high- Λ_{cl} systems should detect X-rays from most of the systems with observations of only moderately increased sensitivity over the ROSAT observations, and the detected ICM will not be hot ($T_x \lesssim 4$ keV). (2) If $L_x \propto \Lambda_{cl}^{3-4}$, the median predicted bolometric X-ray luminosity for the entire undetected sample is $\sim 10^{43} h_{75}^{-2}$ erg s $^{-1}$, so that deep XMM-Newton EPIC exposures should detect most of this population. On the other hand, significant numbers of non-detections with XMM will suggest that many of these clusters are spurious or are significantly less massive than their estimated richnesses may suggest or that there is an X-ray faint population at these mass scales. (3) The X-ray candidates which are not detected by the matched filter algorithm in the optical images will be revealed to be either false clusters of galaxies (constellations of AGN), moderately distant groups, or distant clusters of galaxies ($z > 1 - 1.2$).

REFERENCES

- Adami, C., et al. 2000, ApJ, 120, 1.
 Akritas, M. G. & Bershad, M. A. 1996, ApJ, 470, 706.

- Akritas, M. & Siebert, J., 1996, MNRAS, 278, 919.
- Arnaud, M., et al. 1992, A&A, 254, 49.
- Bahcall, N. et al. 1977, ApJ, 217, L77
- Bahcall, N. et al. 1981, ApJ, 247, 787.
- Borgani, S., et al. 1999, ApJ, 517, 40.
- Couch, W. J., et al. 1991, MNRAS, 249, 606.
- David, L. et al. 1993, ApJ, 412, 479.
- Ebeling, H. et al. 1997, ApJ, 479, L101.
- Edge, A. C., et al. 1990, MNRAS, 245, 559.
- Edge, A. C. & Stewart, G. C. 1991, MNRAS, 252, 428.
- Gioia, I. M., et al., 1990a, ApJ, 356, L35.
- Gioia, I. M., et al., 1990b, ApJS, 72, 567.
- Gioia, I. M., et al., 2001, ApJ, in press (astro-ph/0102332).
- Gunn, J. E., Hoessel, J. G. & Oke, J. B. 1986, ApJ, 306, 30.
- Henry et al. 1992, ApJ, 386, 408.
- Holden, B. P. et al. 1999, AJ, 118, 2002.
- Hradecky, V. et al. 2000, ApJ, 543, 521.
- Jones, L. R. et al 1998, ApJ, 495, 100.
- Kembhavi, A., Feigelson, E. D., & Singh, K. P., 1986, MNRAS, 220, 51.
- Markevitch, M. 1998, ApJ, 504, 27.
- Nichol, R. C., et al. 1999, ApJ, 521, L21.
- Nichol, R. C., et al. 1997, ApJ, 481, 644.
- Postman, M., et al. 1996, AJ, 111, 615.
- Postman, M., Lubin, L. M., Oke, J. B., 1998, AJ, 116, 560.
- Postman, M., et al. 1998, ApJ, 506, 33.
- Romer, A. K., et al. 2000, ApJS, 126, 209.
- Rosati, P. et al. 1995, ApJ, 445, 11L.
- Rosati, P. et al. 1998, ApJ, 492, L21.
- Rosati, P. et al. 2000, in Large Scale Structure in the X-ray Universe, Santorini, Greece, eds. Plionis, M. & Georgantopoulos, I., atlantisciences (Paris), p.13.
- Scharf, C. A. et al. 1997, ApJ, 477, 79.
- Scharf, C. A., et al. 2000, ApJ, 528, L73.

Vikhlinin, A. et al. 1998, ApJ, 502, 558.

Vikhlinin, A. et al. 2000, in Large-Scale Structure in the X-ray Universe, eds. M. Plionis & I. Georgantopoulos, atlantisciences (Paris), p. 31.

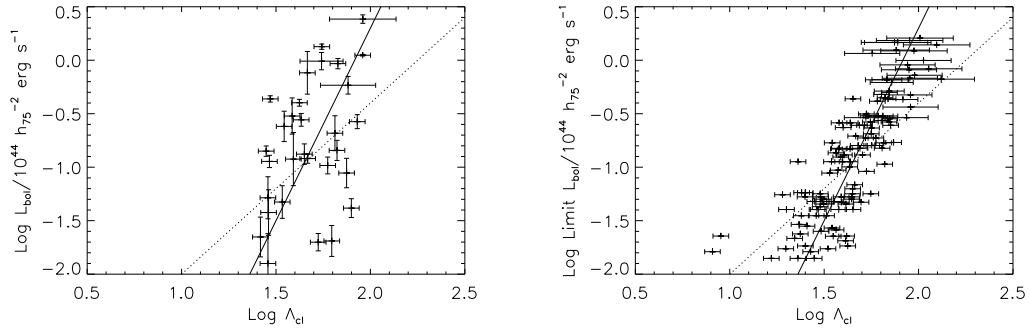


Fig. 1.— We plot bolometric L_x (in units of $\text{Log } 10^{44} h_{75}^{-2} \text{erg s}^{-1}$, for $q_0 = 0.5$) and $\text{Log } \Lambda_{cl}$ for all jointly detected clusters. The dotted line is a best fit to the $L_x - \Lambda_{cl}$ data, where $L_x \propto \Lambda_{cl}^{1.6}$. The solid line represents a best fit obtained in when fit in in conjunction with the Λ_{cl} function and the X-ray luminosity function, where $L_x \propto \Lambda_{cl}^{3.6}$. (The fit parameters are only the normalization of the Λ_{cl} function and the normalization and slope of the $L_x - \Lambda_{cl}$ relation.) On the right hand side, we plot the 4σ upper limits to L_x and the uncertainty on Λ_{cl} , with the same line key as on the right. The moderate bolometric corrections for fluxes in the observed ROSAT bandpass were based on the estimated T_x for the cross-identified candidates and a maximum T_x for the upper limits, iteratively computed from L_x and the $L_x - T_x$ relation from Markevitch (1998).

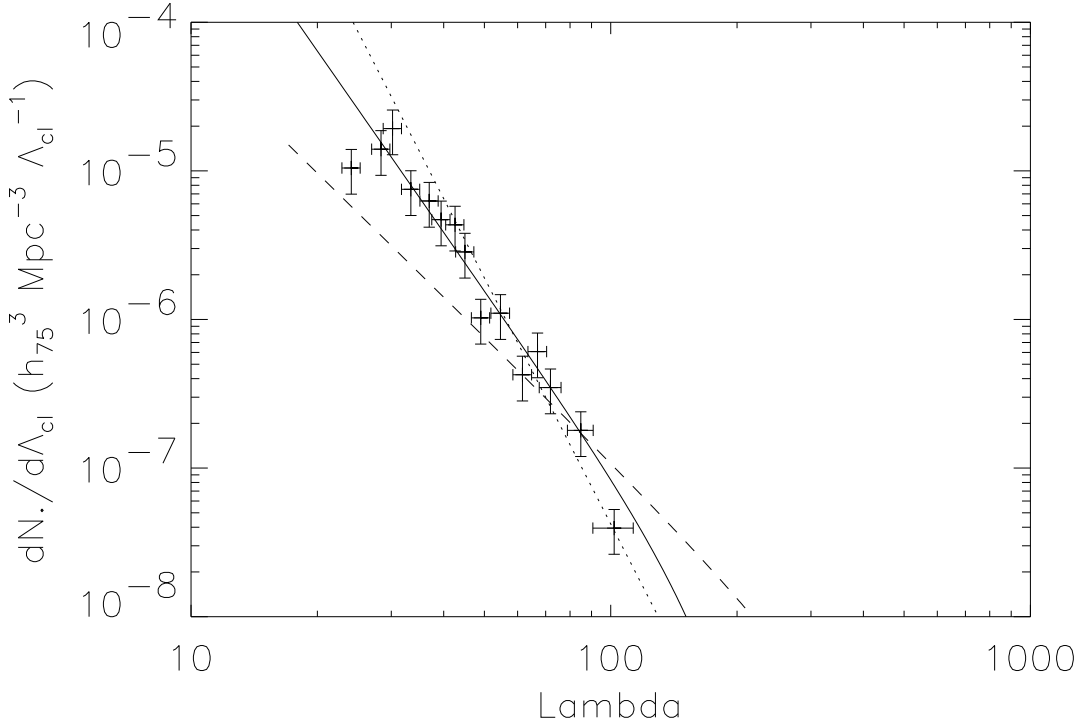


Fig. 2.— Binned differential Λ_{cl} function for the ROXS clusters, with no correction for spurious clusters. The error bars represent the weighted observational uncertainty of the mean Λ_{cl} in that bin of ~ 9 clusters each. The dotted line represents the best fit power-law obtained through a maximum likelihood method for the unbinned sample. The solid line is the best fit Λ_{cl} function as derived from the X-ray luminosity function and the simultaneously fit $\Lambda_{cl} - L_x$ relation with $L_x \propto \Lambda_{cl}^{3.6}$. If $L_x \propto \Lambda_{cl}^{1.6}$, then the inferred Λ_{cl} function is represented by the dashed line. Including moderate scatter changes the normalization but not the slope of these relations. For this plot, we have used $q_0 = 0.5$ and $H_0 = 75h_{75} \text{ km s}^{-1} \text{ Mpc}^{-1}$.